

Confinement Effects and Emission Spectra of $\alpha - Ga_xIn_{1-x}N$ Quantum Dots Nanostructure

Onyekwere O. Ikedichukwu and Oriaku I. Chijioke*

Received: 12 August 2021/Accepted 09 September 2021/Published online: 14 September 2021

Abstract: Quantum confinements in $\alpha - Ga_xIn_{1-x}N$ spherical semiconductor quantum dots (QDs) has been theoretically studied using the Particle in a box Model based on the effective mass approximation and quantum confinement effects. The valence band degeneracy in Γ point of the Brillouin zone and the effective mass anisotropy are also taken into account. The emission intensity spectrum was also investigated to understand the effect of alloy composition (x) on the spectrum. The results show that the ground state confinement energy is largely dependent on radius of the dot and alloy composition (x). Thus, as dot radius decreases, the confinement energy increases. Hence, confinement energies could be tuned by changing the radius of QDs and the GaN compositions, which play a fundamental role in the optical and electronic properties of QDs of all the transitions in the degenerate bands. Also, the theoretically calculated emission intensity spectrum shifted towards higher energy region (lower wavelengths) by mere increasing the alloy compositions (x) of the semiconductor quantum dot active region $\alpha - Ga_xIn_{1-x}N$.

Key Words: Quantum dot nanostructure, quantum confinements, nitride, anisotropic band structure

Onyekwere O. Ikedichukwu

Department of Physics, Michael Okpara University of Agriculture Umudike, P.M.B 7462, Umuahia Abia State, Nigeria

Email: ikedichukwuonyekwere@gmail.com

Orcid Id: 0000-0002-8738-5710

Oriaku I. Chijioke*

Department of Physics, Michael Okpara University of Agriculture Umudike, P.M.B 7462, Umuahia Abia State, Nigeria

Email: oriaku29@gmail.com

Orcid Id:

Communication in Physical Sciences 2020, 7(3):164-173

Available at <https://journalcps.com/index.php/volumes>

1.0 Introduction

Semiconductor quantum dots (SQDs) also known as artificial atoms have attracted much attention for many potential applications due to their unique physical and optical properties such as size-dependent band gap, size-dependent excitonic emission, enhanced nonlinear optical properties and size-dependent electronic properties attributed to quantum size-effect (QSE) (Ahmed *et al.*, 2010; Wei *et al.*, 2014). Past few decades has witnessed the substantial expansion of Group III-nitride semiconductors (Xue *et al.*, 2008). Most of the interest in nitride-based alloys and devices has been on their unique benefit in short-wavelength lights, high-power electrical devices, wide band gap ranging from Infrared to ultraviolet frequencies which are appropriate for electronic and optoelectronic device applications (Steigerwald *et al.*, 1997; Song *et al.*, 2019). GaN and its alloys, particularly InGaN have been proved to be most promising materials for optical devices (Schubert *et al.*, 2008).

Although some dynamic improvement has been actualized in the study of Nitride based devices, numerous fundamental characteristics are still unclear or uninvestigated. For example, knowledge on the quantum confinements in wurzite Nitride QDs that takes full account of the existing anisotropy in the effective masses which is essential for understanding the behaviour of the confined particles has not yet been reported.

Quantum confinement is a unique characteristics of QDs as it transforms the density of states near the band edge (Bera *et al.*

al., 2010 and Eric *et al.*, 2019). With this transformation in the density of electronic states (Wei, *et al.*, 2014), size quantization of exciton states shifts the band gap energy and emission spectrum which is a function of quantum dot sphere's radius (Efros, 1982). This shifts changes the energy levels from continuous to discrete levels (Robinson *et al.*, 2005, Imran *et al.*, 2018 and Khan *et al.*, 2018).

In this paper, quantum confinement effects in spherical $\alpha - Ga_xIn_{1-x}N$ semiconductor quantum dots are theoretically investigated within the framework of a particle in a box model. A method that takes full account of the existing anisotropy in the dielectric constants, electron and hole effective masses and also taking into consideration the valence band degeneracies is discussed. The band parameters obtained in this method are used as inputs in the calculations of the confinement energies and photon emissions are these are discussed in terms of alloy composition and quantum dot radius.

1.1 Theory

The particle in a box model describes the free movement of a particle in a small space surrounded by impenetrable barriers according to Samrat, (2014), the ground state energy of a particle trapped in a spherically symmetric box with $V(r) = \infty$ outside and a constant zero potential energy $V(r) = 0$ inside is found by solving the radial part of the Schrodinger equation:

$$\frac{1}{r^2} \frac{d}{dr} \left(r^2 \frac{dR_l(r)}{dr} \right) + \left(\frac{2m}{\hbar^2} - \frac{l(l+1)}{r^2} \right) R_l(r) = 0 \quad (1)$$

where M is the mass of the particle, $\hbar = \frac{h}{2\pi}$, is the reduced Planck constant, $R_l(r)$ is the eigen function of the eigen energy E with l representing the orbital angular momentum of the particle quantum state. The application of the boundary condition, ($R_l(r) = 0$ for $r = a$ where $V(r) \rightarrow \infty$) leads to the simplification of equation 1 to generate equation 2

$$R_0(r) = \frac{B \sin kr}{r} \quad (2)$$

where B is the normalization constant. Also, the ground state energy of a particle confined in a one dimensional box can be written as follows:

$$E_0 = \frac{h^2}{8m^2} \quad (3)$$

The modification of equation 3 to contain the energies corresponding to each of the allowed wavenumbers

associated with the respective principal quantum number leads to equation 4

$$E_n = \frac{n^2 h^2}{8m^2 r^2} \quad (4)$$

Equation 4 is an extension of the Schrödinger equation that is best referred to as, the particle in a box model. The mathematical implication of equation 4 is that the energy of a particle will always assume a non-zero value. This model can be applied to analyse the quantum dot problem, since in quantum dot, electrons and holes are typically confined within the dots (Efros, 1996). The extension of the one the particle in a box problem to account for the masses of electrons and hole gives the solution to the theoretical energy expected within the quantum dot according to the form expressed in equation 5 while equation 6 represents the ground state confinement energy of electrons and holes in the quantum dots.

$$E = \frac{nh^2}{8m_e^* R^2} + \frac{nh^2}{8m_h^* R^2} \quad (5)$$

$$E = \frac{h^2}{8R^2} \left(\frac{1}{m_e^*} + \frac{1}{m_h^*} \right) \quad (6)$$

m_e^* and m_h^* are the effective masses of electron and hole respectively. In Wurtzite Structures, the reduced mass, $\mu = m_e m_h / (m_e + m_h)$ and static dielectric constant $\epsilon(0)$ arising from the structural anisotropy can best be approximated to the forms expressed by Hanada *et al.* (2013) as follow:

$$\frac{1}{m_e} = \frac{2}{3m_e^{\parallel}} + \frac{\epsilon^{\perp}(0)}{3\epsilon^{\parallel}(0)m_e^{\parallel}}$$

$$\frac{1}{m_h} = \frac{2}{3m_h^{\parallel}} + \frac{\epsilon^{\perp}(0)}{3\epsilon^{\parallel}(0)m_h^{\parallel}}$$

Also, the average statistical dielectric constant $\epsilon(0)$ can be written as equation 9, (Hanada *et al.* (2013)):

$$\epsilon(0) = \sqrt{\epsilon^{\parallel}(0)\epsilon^{\perp}(0)}$$

where $\epsilon^{\parallel}(0)$ and $\epsilon^{\perp}(0)$ are static dielectric parallel and perpendicular respectively, $m_e^{\parallel}, m_e^{\perp}, m_h^{\parallel}, m_h^{\perp}$ are the effective masses of electron and hole parallel and perpendicular respectively. Consequently, the energy gap of a quantum dot can be written as follows (Efros, 1996):

$$\Delta E(R) = E_g + \frac{h^2}{2R^2} \left(\frac{1}{m_e^*} + \frac{1}{m_h^*} \right) \quad (10)$$

The bandgap, E_g of the ternary alloy can be interpolated from the bandgap of the constituent binary alloy using the quadratic function (equation 11):

$$E_g(x) = (1-x)E_g^{AC} + xE_g^{BC} - bx(1-x) \quad (11)$$

where E_g is bandgap of the bulk wurtzite semiconductor material being studied, x is the alloy composition, and b is the bowing parameter.



2.0 Absorption spectra of the structure

The linear optical absorption, α at a given frequency ω can be investigated using a very simple phenomenological formula of the type expressed in equation 12 (Osuwa, and Oriaku, 2010, Oriaku and Osuwa, 2009, and Pelant and Valenta, 2012), etc.,

$$\alpha(\omega) = \frac{A(\hbar\omega - \Delta E(R))^n}{\hbar\omega} \forall \hbar\omega > E_g \quad (12)$$

In equation 12, ω and \hbar denote the incident sample photon frequency and the reduced Planck's constant respectively. A is the material parameter to be extracted from the semiconductor.

2.1 Emission intensity spectra of the structure

Also, the band-to-band contribution to the semiconductor photoluminescence intensity can be expressed as follows (Yanlin H. and Hyo J. S. 2012):

$$I(\omega) = A((\hbar\omega - \Delta E(R))^n \left[\frac{1}{e^{\beta(\hbar\omega - \Delta E(R))}} \right]) \forall \hbar\omega > E_g \quad (13)$$

Here β is simply the inverse thermal energy given as $1/k_B T$, where k_B and T are the Boltzmann's constant and temperature. The band parameters adopted in the calculations are summarized in Table 1.

Table 1: Parameters used in modeling the Tunable Exciton Energies of WZ-GaInNQDs.

Material	E_g (eV)	m_e^{\parallel}	m_e^{\perp}	m_{hh}^{\parallel}	m_{lh}^{\parallel}	m_{ch}^{\parallel}	m_{hh}^{\perp}	m_{lh}^{\perp}	m_{ch}^{\perp}	$\epsilon^{\parallel}(0)$	$\epsilon^{\perp}(0)$
GaN	3.510	0.20	0.18	1.10	1.10	0.15	1.65	0.15	0.10	9.5	10.4
InN	0.78	0.11	0.10	1.67	1.67	0.10	1.61	0.11	1.67	15.0	15.0

(Source: Hanada, 2013)

3.0 Results and Discussion

The effects of composition x on the anisotropic electron effective masses for both parallel (\parallel) and perpendicular (\perp) directions in the dot material were evaluated and the electron effective masses were

observed to increase with composition x increases as shown in Fig. 1. This result is in accord with the observation reported by Zhou and Sheng (2008) for flat InAs/Ga-As quantum dot.

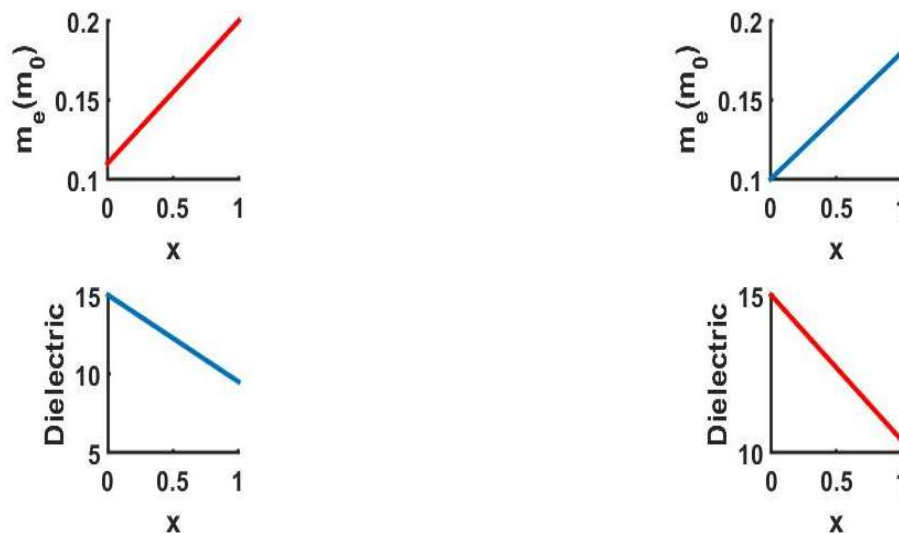


Fig. 1: Variation of dielectric with composition, x for $\alpha - Ga_xIn_{1-x}N$ nanostructure dots
 Figs. .2 and 3 are the plots the variation of hole effective-mass as a function of alloy composition (x). The figures reveals that hole effective-masses for the three holes namely: heavy hole (hh), light hole (lh) and crystal field hole (ch) in the parallel direction was found to be inversely dependent on the alloy composition. A similar characteristic was observed for light hole and crystal field hole in perpendicular plane. The heavy hole in the perpendicular plane displayed direct dependent on the alloy composition. The



effective mass anisotropy of the holes showed unique differences in energy for the various directions with to the C-axis, that is the

splitting of the quantum confinement levels of the holes.

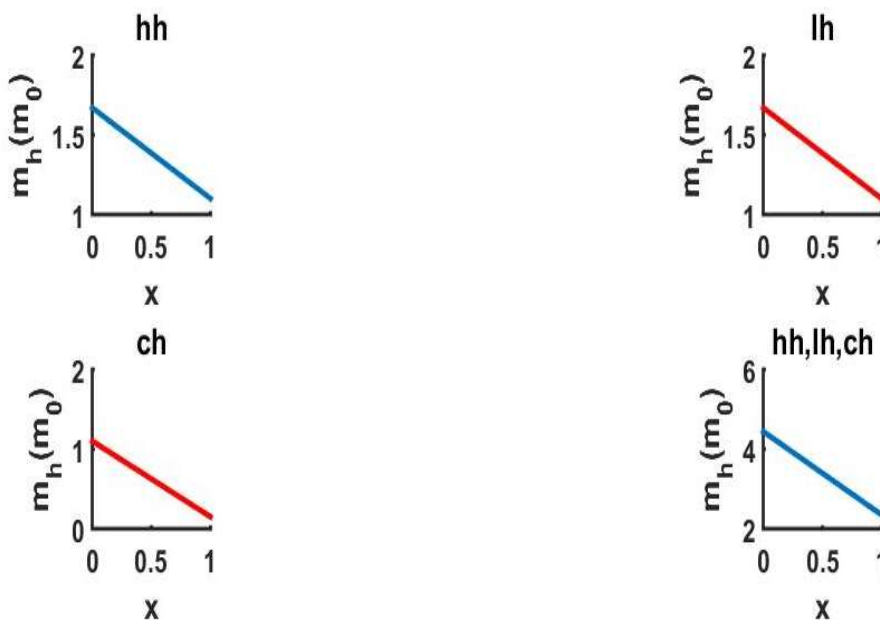


Fig.2: Hole effective mass (\parallel) as a function of composition x

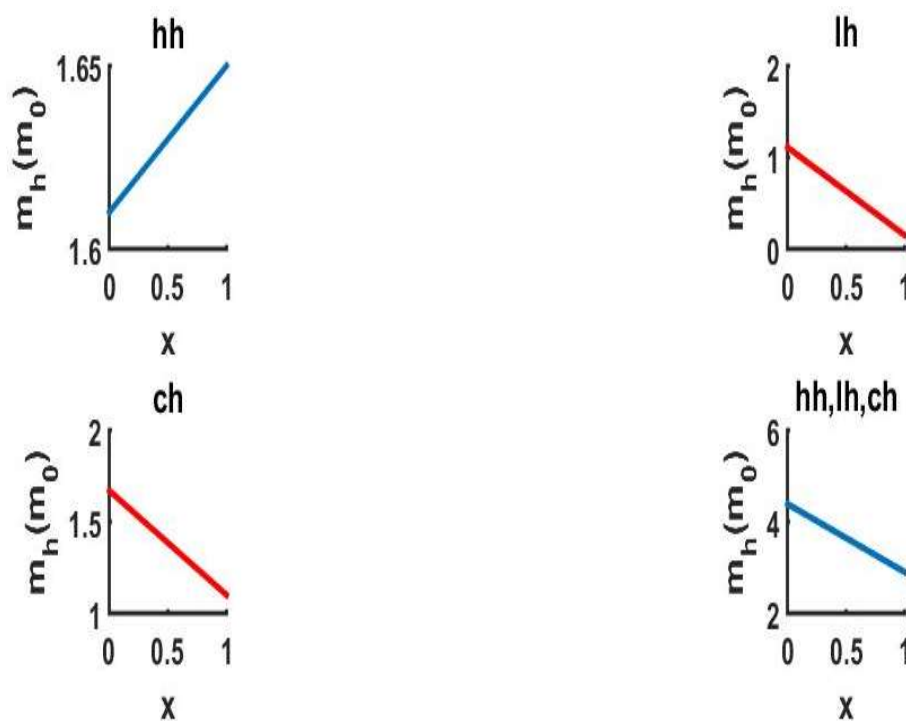


Fig.3: Hole effective mass (\perp) as a function of composition x



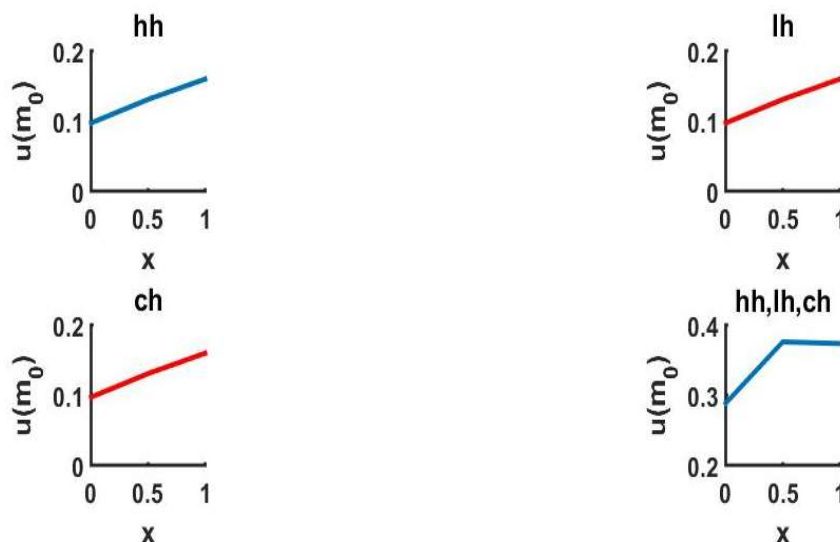


Fig.4: Reduced mass as a function of composition x

We have used Particle in a box model within effective mass approximation to calculate the ground state confinement energy of $\alpha - \text{Ga}_x\text{In}_{1-x}\text{N}$ spherical QDs as a function of dot radius $R=1-8\text{nm}$ and varying alloy composition $x=0.5, 0.75, 1$. The results are as reported here. The conduction and valence band of $\alpha - \text{Ga}_x\text{In}_{1-x}\text{N}$ quantum dot studied is anisotropic. Therefore, effective masses of electrons and holes in parallel and perpendicular directions towards C-axis of the dot are non-identical as shown in Table 1. The $\alpha - \text{Ga}_x\text{In}_{1-x}\text{N}$ quantum dot

confinement energy show clear dependence on dot radius at different alloy composition(x) in all the plots for the respective subbands. It is clearly observed that the decrease of the dot radius shifts the energy levels. These shifts are considerably dependent on alloy composition(x) and effective masses of the carriers. The larger is the composition(x), the larger is the shift. Thus revealing the ability of $\alpha - \text{Ga}_x\text{In}_{1-x}\text{N}$ quantum dot to be tuned within energies ranging from about 1.5eV to 5.5eV covering the Infrared to UV spectral range (Figs.5 to 7).

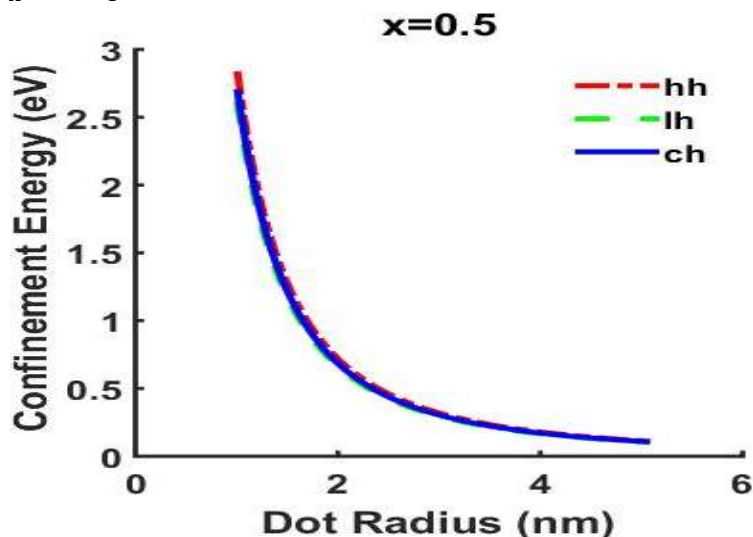


Fig.5: Confinement energy at x=0.25 composition as a function of dot radius



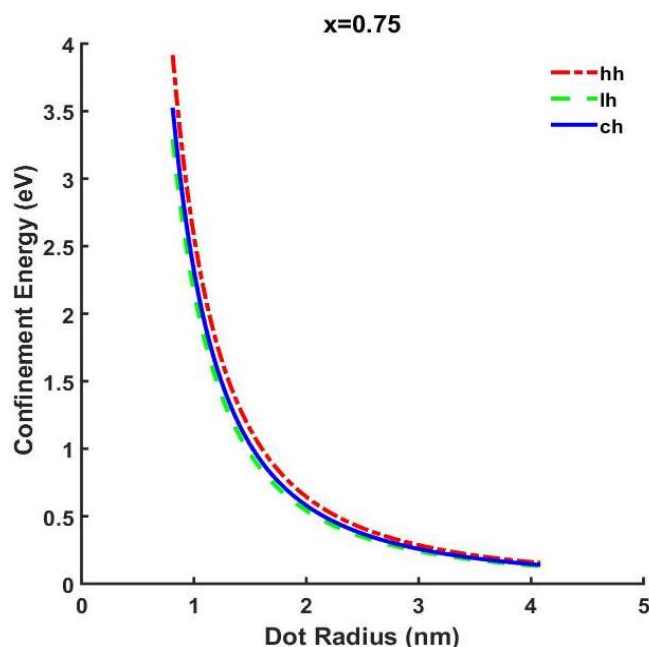


Fig.6: Confinement energy at x=0.75 composition as a function of dot radius

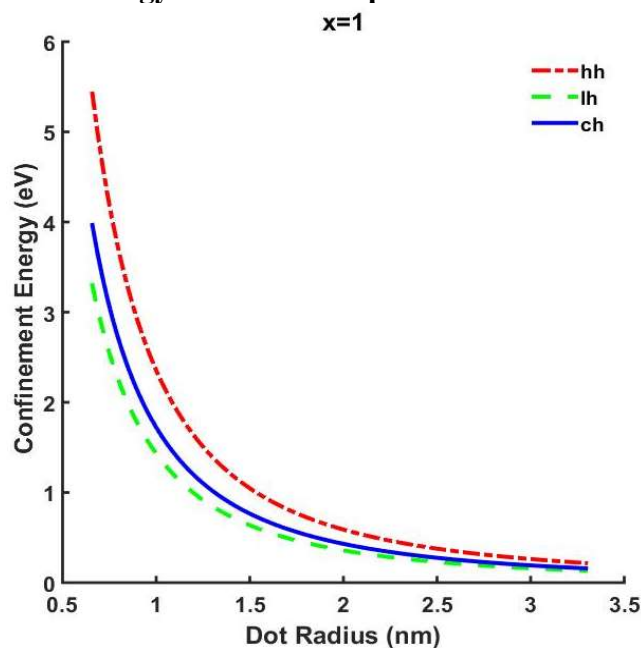


Fig.7: Confinement energy at x=1 composition as a function of dot radius

Quantum dot Emission Intensity
 Figs. 8 to 10 are plots for the emission intensity of $\alpha - \text{Ga}_x\text{In}_{1-x}\text{N}$ quantum dot at different alloy composition(x). It is evident from the plots that the intensity manifested as a broad signal, which may be attributed to the inhomogeneous broadening due to different alloy composition(x). Calculations of the

intensity at different composition (x) indicated that the observable shift in intensity increase with alloy composition (x). A similar observation has been for GaN/AlN structures (Rami, 2011). Therefore, the signal is influenced by varying alloy composition. At x



=0.75 in Fig. 8, three sharp peaks were observed at around 4.0eV, 4.5eV and 4.8eV respectively depicting the emission intensity at hh, lh, chsubbands respectively. These peaks are believed to be emission signal from

the binary structures due to their broad spectrum. Thus, the intensity desired for optical devices can be realized by varying the alloy composition(x).

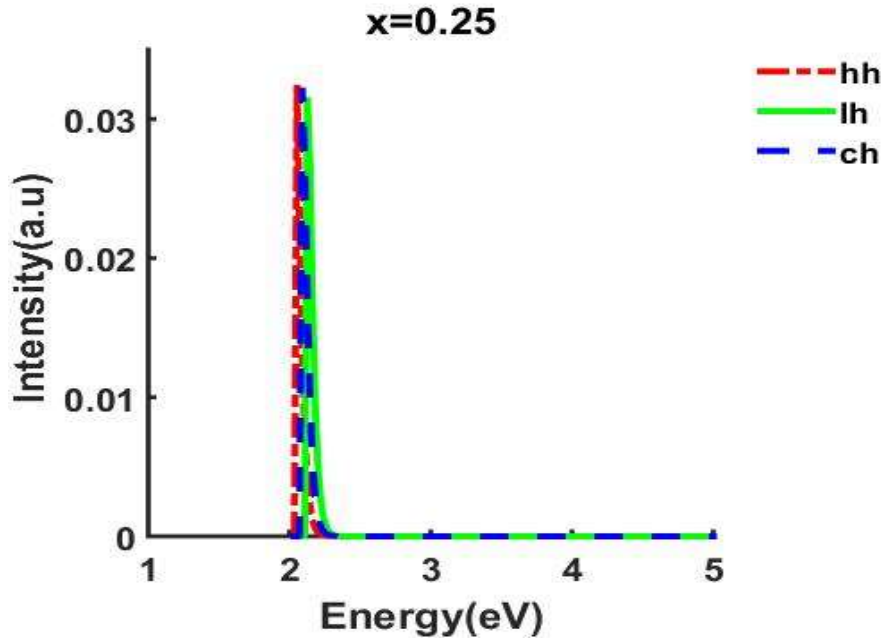


Fig.8: Emission intensity of hh, lh, chsubbands at 0.25 composition(x) as a function of photon energy in $\alpha - \text{Ga}_x\text{In}_{1-x}\text{N}$ QD.

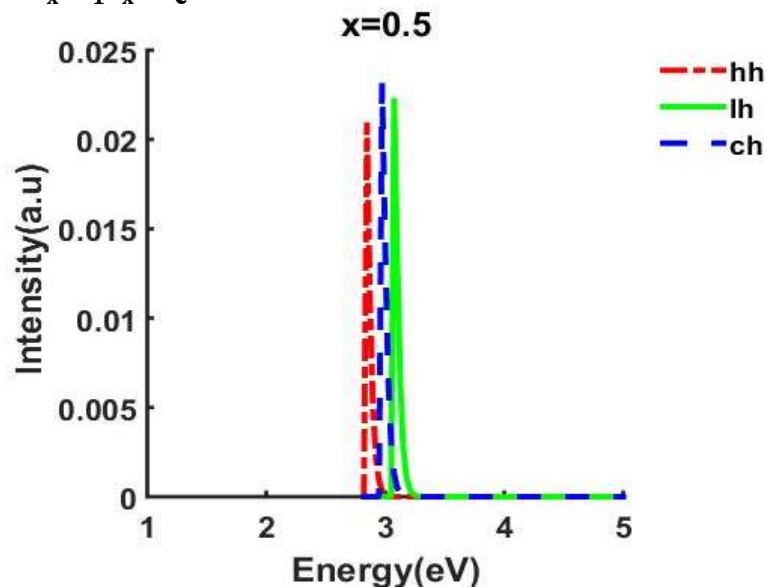


Fig.9: Emission intensity of hh, lh, chsubbands at 0.5 composition(x) as a function of photon energy in $\alpha - \text{Ga}_x\text{In}_{1-x}\text{N}$ QD.



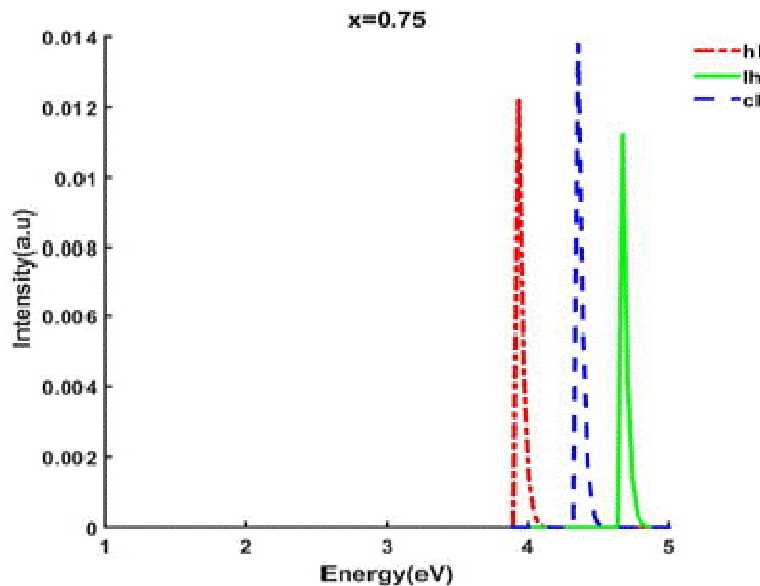


Fig.10: Emission intensity of hh, lh, ch subbands at 0.75 composition(x) as a function of photon energy in $\alpha - \text{Ga}_x\text{In}_{1-x}\text{N}$ QD

The most important factor that affects the optical properties is the size of the dots. Different sized quantum dots change the color emitted or absorbed by the crystal, due to the energy levels within the crystal. It is evident from the results presented in Table 2 that the emission spectrum, the color of the light differs according to the energy emitted by the crystal. Red light is associated with lower energy while blue light is associated with a

higher energy. Also, the size of a quantum dot is inversely proportional to the band gap energy level, and therefore alters the wavelength of light emitted and has an effect on the color it displays. Smaller dots emit higher energy light that is bluer in color, whereas larger dots emit lower energy red light. The size of the dot can be manipulated in manufacturing processes by varying the material composition as done in this work to create a quantum dot suitable for specific optical devices.

Table 2: Emission wavelength of different degenerate bands at different composition, x

Degenerate holes	Composition(x)	Emission Energy(eV)	Emission colour
hh	0.25	2.2	Red,orange
	0.5	2.8	Green,Blue
	0.75	3.9	Blue
lh	0.25	2.1	Red,orange
	0.5	3.0	Green,Blue
	0.75	4.5	Blue
ch	0.25	2.0	Red,orange
	0.5	3.3	Green,Blue
	0.75	4.8	Blue



4.0 Conclusion

In conclusion, we have investigated theoretically quantum confinement in $\alpha - Ga_xIn_{1-x}N$ spherical semiconductor quantum dot. We showed how different valence subbands of $\alpha - Ga_xIn_{1-x}N$ can change the dynamics of the QD and create different responsivity toward alloy compositions(x) and dot radius. It is clearly observed that the decrease of the dots shifted the energy levels from 1.5eV to 5.5eV. These shifts are considerably dependent on alloy composition(x) and effective masses of carriers. The larger is the composition(x), the larger is the shift. Besides, the degeneracies of the holes confinement energies are distinctly observed at some values of R and x for the different valence subbands. Furthermore, the emission intensity spectrum of the quantum dot material studied shifted towards higher energies by increasing alloy composition(x). The QD material studied exhibited confinement at around the orange/red domain, mainly due to the Indium composition, the confinement spectrum also shifted towards the blue domain by incorporating Gallium. This would make it possible to create efficient solid state white light.

5.0 References

- Ahmed, S. & Mohammed, S. (2010). Electronic Structure of InN/GaN Quantum Dots: Multimillion-Atom Tight-Binding Simulations. *IEEE Transactions on Electron Devices*, 57, 1, pp. 164 – 173..
- Bera, D., Qian, L., Tseng, T.K. *et al.* (2010). Quantum Dots and Their Multimodal Applications: A Review, *Materials*, 3, 4, pp. 2260-2345.
- Efros, A. L. (1996). Band-edge Exciton in Quantum Dots of Semiconductors with a Degenerate Valence Band. *Phys. Rev. B*, Vol. 54, No. 7, 4843.
- Eric, D. *et al.* (2019). Optical properties of InN/GaN quantum dot superlattice by changing dot size and interdot spacing, *RIP*, 13, 102246.
- Hanada, T. (2013). Basic Properties of ZnO, GaN, and Related Materials. *Journal of Applied Physics*. pp1-19.
- Imran, A. *et al.* (2018). Size and shape dependent optical properties of InAs quantum dots.
- Khan, A. *et al.* (2018). Solution Processed Trilayer Structure for High-Performance Perovskite Photodetector, *Nanoscale Res Lett*, 13(1), 399.
- Kunets V.P (1999). Model of optical transitions in wurzite type quantum dots. *Journal of Semiconductor physics*. vol.2, pp.22-27.
- Osuwa, J.C and Oriaku C.I (2010). Laser induced changes on band gap and optoelectronic properties of chalcogenide glassy $Cu_{0.11}Cd_{0.40}S_{0.49}$ thin films. *Journal of Non-Oxide Glasses*, 2, pp. 1-5.
- Oriaku, C.I and Osuwa, J.C (2009). On the optical dispersion parameters of thin film Al₃ doped ZnO transparent conducting glasses. *Journal of Ovonic Research*, 5, 6, pp. 213-218.
- Pelant, I. and Valenta, J. (2012). *Luminescence Spectroscopy of Semiconductors*. Oxford Press.
- Robinson, J. W. *et al.* (2005). Quantum-confined Stark effect in a single InGaN quantum dot under a lateral electric field, *App Phys. Lett.*, 86(21), 213103.
- Schubert, M. F. *et al.* (2008). Polarization-matched GaInN/AlGaInN multi-quantum-well light-emitting diodes with reduced efficiency droop. *App Phys. Lett.*, 93(4), 041102.
- Song, C. *et al.* (2019). Impact of Silicon Substrate with Low Resistivity on Vertical Leakage Current in AlGaIn/GaN HEMTs.
- Steigerwald, D. *et al.* (1997). III-V Nitride Semiconductors for High Performance Blue and Green Light Emitting Devices, JOM. University Press; New York.
- Wei, J. *et al.* (2018). β -Ga₂O₃ thin film grown on sapphire substrate by plasma assisted



- molecular beam epitaxy. *Journal of Semiconductor*, **40**, 012802.
- Yanlin H. and Hyo J. S. (2012). Luminescence Properties and Refractive-Index Characterization of Li+-Doped PbWO₄ Single Crystals. *J. Korean Phys. Soc.* Vol. 50, No. 2, pp. 493 - 499.
- Zhou, A.P. and Sheng, W.D (2008). Electron and hole effective masses in self-assembled quantumDots. *The European Physical Journal B*. DOI: [10.1140/epjb/e2009-00098-2](https://doi.org/10.1140/epjb/e2009-00098-2).

Conflict of Interest

The authors declared no conflict of interest

